Journal of Physics: Conference Series **682** (2016) 012003 doi:10.1088/1742-6596/682/1/012003

Plasmonic thin films for application in improved chromogenic windows

Gunnar A Niklasson[1], Pia C Lansåker, Shu-Yi Li and Claes G Granqvist

Department of Engineering Sciences, The Ångström Laboratory, Uppsala University, P.O. Box 534, SE-75121 Uppsala, Sweden

[1]E-mail: gunnar.niklasson@angstrom.uu.se

Abstract. Nanocomposites consisting of noble metal nanoparticles in a transparent matrix exhibit plasmonic absorption in the visible wavelength range, and conducting oxide nanoparticles display a localized plasma absorption in the near infrared. The optical properties of nanocomposites are commonly modelled by effective medium theories, which describe the effective dielectric function of the composite using as input the dielectric functions of the constituents and their respective volume fractions. Plasmonic effects can be exploited in the design of energy-efficient windows in order to obtain improved performance. Electrochromic coatings that switch in the near infrared make use of the modulation of the plasma absorption of oxide nanoparticles due to charge density modulation induced by an external voltage. Plasmonic thermochromic switching in the near infrared has the potential to be significantly larger than in the case of a thin film. Very thin noble metal films are an interesting alternative to conducting oxides as transparent contacts to electrochromic devices. However, in this latter case plasmonic effects are to be avoided rather than exploited.

1. Introduction

The optical properties of nanoparticles, in particular effects related to the localized plasma resonance of metallic particles, have recently attracted major interest. Applications include sensors and biosensors [1,2], as well as plasmonic enhancement of photocatalysis [3-5]. In the field of renewable energy, applications to solar cells [6–8] and highly absorptive films for solar harvesting [9] have been proposed. The scientific study of plasmonic effects has a long pre-history, at least dating back to theoretical and experimental studies of the optical properties of noble metal nanoparticles in the early twentieth century [10,11].

Many studies have concerned noble metal nanoparticles and the dependence of the localized plasma absorption peak on particle shape and surroundings [12], substrate effects [13] and non-locality of the dielectric response [14] has been elucidated. Recently there has emerged a rising interest in alternative plasmonic materials such as TiN [15], other metal oxides and nitrides [16], alloys and intermetallics [17]. In particular oxide-based plasmonic materials exhibit their localized plasma absorption in the near-infrared (NIR) spectral range, thereby opening up a number of new applications.

In this paper we review recent work on coatings for energy-efficient windows, which take advantage of plasmonic effects. Section 2 below gives a basic theoretical background of the subject. Section 3 reviews the optical properties of ultrathin gold films and their application as transparent conductor coatings. Section 4 reviews the subject of plasmonic electrochromism, wherein the plasma resonance of highly doped oxide semiconductor nanoparticles can be tuned by an electrical signal.

Finally, section 5 demonstrates that plasmonic effects play an essential role for the enhanced thermochromism in VO_2 nanoparticle composites.

2. Localized plasma resonance

In this section we give an introduction to the theory of plamonic absorption, but first we recall briefly some basic facts about the optical properties of metals. The optical properties of metallic materials can be approximately described by a dielectric function of the Drude form, namely [18]

$$\varepsilon_f(\omega) = 1 - \omega_p^2 / (\omega(\omega + i/\tau)), \tag{1}$$

where ω_p is the plasma frequency of the free electrons and τ is the relaxation time that describes electron scattering by phonons, defects, impurities and, in the case of nanoparticles, most importantly scattering against the particle surface. This expression only accounts for the optical properties due to the conduction electrons and, in the case of real metals, terms describing interband absorption have to be added [18]. For metal oxide based plasmonic materials, the picture becomes more complicated and the relaxation time becomes in general frequency dependent [19]. The reason is that these materials are heavily doped oxide semiconductors and scattering of conduction electrons from charged impurities, *i.e.*, the dopant ions, is very important. In this case eq. (1) has to be replaced by a Lindhard dielectric function [20] with further refinements, as described in detail by Hamberg and Granqvist [21].

The measurable optical properties are reflectance (R) and transmittance (T), from which absorption, $A = 1 - T - R$, can be obtained. The transmittance and reflectance can be computed from the dielectric function by thin film optics [22]. The absorption is related to the imaginary part of the dielectric function. A maximum in that quantity implies an absorption peak, which is visible as a dip in the transmittance of a thin film.

2.1. Effective medium theory

The optical properties of nanoparticles in an embedding matrix are described by the effective dielectric function, ε^{eff}, of the composite. The relation between this function and the dielectric functions of the constituents is provided by effective medium theories. Here we use to the Maxwell Garnett theory [10], which is appropriate for a topology with spherical nanoparticles dispersed in a continuous matrix. Specifically,

$$\varepsilon^{eff}(\omega) = \varepsilon_m\left(\varepsilon_p + 2\varepsilon_m + 2f\left(\varepsilon_p - \varepsilon_m\right)\right)/\left(\varepsilon_p + 2\varepsilon_m - f\left(\varepsilon_p - \varepsilon_m\right)\right), \tag{2}$$

where ε_m is the dielectric function for the matrix material and f is the volume fraction occupied by the particles. The dielectric function of the particles, ε_p, is obtained from ε_f by modifying the relaxation time to account for scattering of electrons from the surfaces of the particles. It must be understood that the dielectric functions in general are frequency dependent, although it is not written explicitly in the case of ε_p and ε_m. We now insert eq. (1) into eq. (2) and obtain the Lorentz oscillator form of the effective dielectric permittivity [23],

$$\varepsilon^{eff}(\omega) = \left(\omega_L^2 - (\omega(\omega + i/\tau)\right)/\left(\omega_T^2 - (\omega(\omega + i/\tau)\right), \tag{3}$$

where the effective longitudinal and transverse resonance frequencies are given by [23]

$$\omega_L^2 = \omega_p^2(1 + 2f)/(1 + 2f + 2\varepsilon_m(1 - f)) \tag{4}$$

and

$$\omega_T^2 = \omega_p^2(1-f)/(1-f+\varepsilon_m(2+f)). \tag{5}$$

The maximum of the optical absorption occurs at the transverse resonance frequency, and in the limit of low volume fraction and $\varepsilon_m = 1$, we obtain the well-known result $\omega_p/\sqrt{3}$. Hence Drude metallic particles dispersed in a matrix gives rise to localized plasma absorption at the transverse resonance frequency given by eq. (5) above. For noble metal particles, this frequency falls in the visible wavelength range, while for highly doped semiconductors and VO_2, which exhibit a much lower plasma frequency, the resonance frequency falls in the NIR.

2.2. Ellipsoidal particles

In the case of ellipsoidal particles the expressions above have to be generalized and it is convenient to rewrite the MG effective dielectric function in the form [24]

$$\varepsilon^{eff}(\omega) = \varepsilon_m\left(1+\frac{2}{3}f\alpha\right)/\left(1-\frac{1}{3}f\alpha\right) \ . \tag{6}$$

For oriented ellipsoids with the incident electric field along the *j*-axis one obtains

$$\alpha = \frac{\varepsilon_p - \varepsilon_m}{\varepsilon_m + L_j(\varepsilon_p - \varepsilon_m)} \ , \tag{7}$$

where L_j is the appropriate depolarization factor. Spheres are characterized by $L = ⅓$, and in this case eq. (2) is obtained again. A random distribution of ellipsoidal particles can be described by [24]

$$\alpha = \frac{1}{3}\sum_{i=1}^{3}\frac{\varepsilon_p - \varepsilon_m}{\varepsilon_m + L_i(\varepsilon_p - \varepsilon_m)} \ , \tag{8}$$

where the L_is are a triplet of depolarization factors. A spheroid exhibits two localized plasma resonances, while a general ellipsoid exhibits three, one for each value of the depolarization factor L_i.

2.3. Spectral density function

We have seen that non-spherical shapes introduce more than one localized plasma resonance. More complex shapes than the ellipsoidal, together with dipolar and multipolar interactions between the electromagnetic fields scattered by particles close to one another, leads to a spectrum of resonances. By introducing a spectral density function (SDF), *g(x),* we can write the effective dielectric function in a completely general way, which is valid for all conceivable distributions of particle shapes, local densities as well as for separated and touching particles [25,26]:

$$\varepsilon^{eff} = \varepsilon_m\left(1+\int_0^1 \frac{g(x)}{((\varepsilon_p/\varepsilon_m)-1)^{-1}+x}dx\right). \tag{9}$$

The Maxwell-Garnett theory for spheres, eq. (2), corresponds to $g(x)$ being a δ-function positioned at $(1-f)/3$. It is a very complex problem to determine the SDF by inverting experimental optical measurements. However, recent advances have made it manageable and hence it is possible to analyze the spectrum of localized plasma resonances for samples with a very complex nanostructure [27,28].

3. Ultrathin gold films as transparent contacts

Transparent conducting coatings are needed in a variety of applications including displays, solar cells, low-emittance window coatings and electrochromic devices [29]. Highly doped semiconductors, for example doped indium, tin or zinc oxides, are currently used in most of these applications [29]. Thin silver films are used in dielectric/metal/dielectric (D/M/D) stacks as low-emittance coatings. However, Ag films exhibit durability problems when used in displays and electrochromics, and here gold is a more rugged alternative.

Thin films of Au and TiO_2 were prepared by DC magnetron sputtering onto unheated glass substrates from metallic targets. The Au deposits had mass thicknesses (equivalent thicknesses in the absence of porosity) in the 1.4–9.8 nm range, as inferred from deposition rate. Spectral normal transmittance, $T(\lambda)$, was measured in the wavelength range 0.3–2.5 μm using a Perkin-Elmer Lambda 900 double-beam spectrophotometer. Figure 1 shows data for Au films with nine different thicknesses [30]. There is a consistent pattern at NIR wavelengths, namely $T(\lambda)$ decreases monotonically with increasing film thickness. The localized plasma absorption is visible as a dip in the transmittance for the two thinnest films at $\lambda \sim 0.6$–0.7 μm. The flat NIR transmittance for films of thicknesses being 4–5 nm indicates a transition from a dielectric nanoparticle film to a metallic network film and coincides with a transition to a high electrical conductivity. Au films are almost completely continuous at a thickness of 10 nm.

The effective dielectric function of the Au films was obtained from ellipsometry, as described elsewhere [31], and subsequently the SDF was obtained by advanced computational methods devised by Tuncer [27,28,31]. Figure 2 shows the SDF for three gold films. A nanoparticle film with mass thickness 1.4 nm shows a well-defined resonance that is somewhat broadened by interaction effects towards lower x. On the other hand network films exhibit a SDF extending all the way from the MG resonance to $x = 0$ [31]. Hence part of the absorption strength is for these films displaced towards long wavelengths, as evident also from figure 1. The third sample in figure 2 is an almost continuous film; $g(x)$ displays very low values, probably as a result of nano-holes in the film.

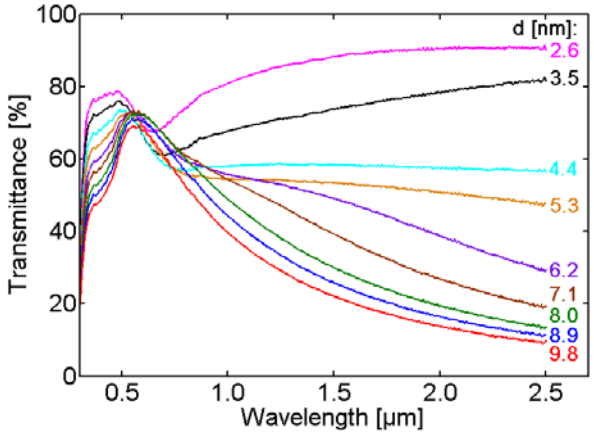

Figure 1. Spectral transmittance of gold films with the shown thicknesses d, made by sputtering onto glass. From [30].

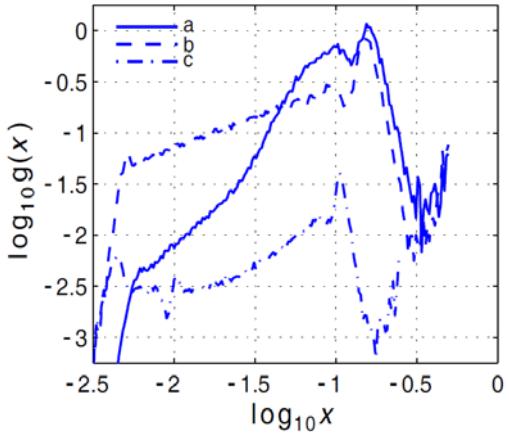

Figure 2. Spectral density function for ultrathin gold films with mass thicknesses (a) 1.4 nm, (b) 3.8 nm and (c) 9.2 nm. From [31].

The requirements for a transparent conductor are high transmittance and good electrical conductivity. In applications demanding high solar transmittance, metallic network films are advantageous but a trade-off has to be made with requirements of conductivity and durability. The visible transmittance in figure 1 is somewhat low for window applications, especially in the case of an

electrochromic "smart" window which must include two transparent conductors. However, the transmittance can be increased by incorporating the Au film in a D/M/D stack. Figure 3 shows that the transmittance of a thin Au film can be considerably enhanced by having it between two TiO_2 coatings. It is seen that the transmittance reaches 80% in the mid-visible range.

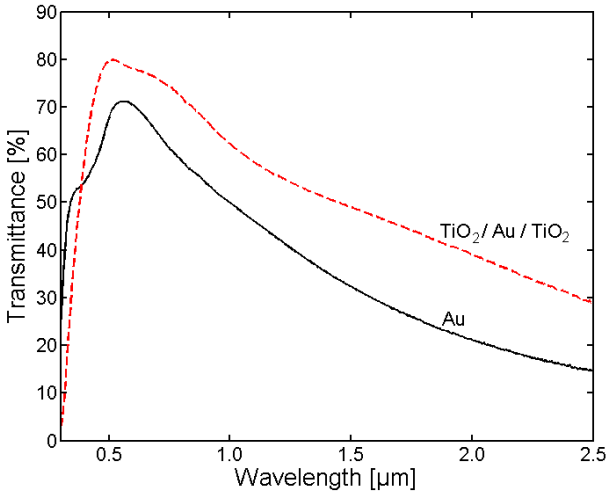

Figure 3. Spectral transmittance for an 8.0-nm-thick Au film and a TiO_2/Au/TiO_2 stack with 8 nm Au and 55-nm-thick TiO_2 films. From [30].

In order to evaluate D/M/D stacks for electrochromic applications, electrochemical cycling tests were performed with the optimized TiO_2/Au/TiO_2 film, backed by glass, immersed in an electrolyte of 0.5M $LiClO_4$ in propylene carbonate and sweeping the voltage between 3 and 5 V with regard to a Li reference electrode at a rate of 1 mV/s [30]. The Au-based film was found to remain unaffected for at least 20 cycles. For comparison, we performed an identical test with a commercial Ag-based D/M/D type transparent conductor, which revealed a prominent oxidation peak already during the first electrochemical cycle; this oxidation degrades this film severely and turns it into a non-conductor. Hence gold-based films are sufficiently stable so that they can be used as transparent conductors in demanding environments. The dielectric layers in the D/M/D stack must have a not too high resistance, although the requirements are not as strict as for an all-oxide-based transparent conductor. In real applications, doped oxide layers with moderately high conductivity would have to be used.

4. Plasmonic electrochromism

A new approach to electrochromism was developed by Milliron *et al*. [32] who demonstrated that transmittance modulation in the NIR can be achieved electrochemically in layers with nanoparticles consisting of a transparent and electrically conducting material such as In_2O_3:Sn (ITO). This opens up possibilities to use plasmonic effects, rather than polaron effects as in many electrochromic transition metal oxides [33,34], in order to produce a significant modulation of the solar energy transmittance. Furthermore, inclusion of ITO nanocrystals into a film of niobium oxide glass allowed independent modulation of the visible and near-infrared transmittance by changing the applied electrochemical potential [35].

The effect responsible for plasmonic electrochromism in transparent conducting oxide particles is that the localized plasmon frequency of, for example, ITO nanoparticles can be persistently and reversibly tuned electrochemically. The application of different potentials to a nanoparticle film modulates the charge carrier density, and hence the plasma frequency, most probably by the creation of dynamic accumulation and depletion layers at the nanoparticle surfaces [32]. Thus the localized plasma resonance absorption can be swept through the NIR so that a variable part of the solar radiation

is absorbed, while the luminous absorption remains high. ITO films can display electron densities as high as ~2.5 × 10^{21} cm^{-3} [29], and similar values have been reported for ZnO-based films [36]. The corresponding localized plasma absorption lies in the NIR or in the red end of the visible spectrum.

We now present a method to calculate approximate performance limits for the luminous and solar transmittance (T_{lum} and T_{sol}, respectively) [37]. Our starting point is the dielectric function due to the free electrons in the transparent conductor. Charged impurity scattering is inevitable in a highly doped oxide and is taken into account by the theoretical framework summarized in section 2 [19–21]. The optical properties of ITO nanoparticles in a dielectric medium can be calculated by effective medium theory, eq. (2), in combination with thin film optics, and the upper panel of figure 4 shows spectral absorptance for a 5-μm-thick layer of ITO nanoparticles in a medium with ε_m=2.25; this value is characteristic for typical polymers and glasses. It is obvious that the localized plasmon peak moves from long wavelengths to ~1.3 μm when the charge carrier concentration, n_e, is increased to 2 × 10^{21} cm^{-3}. The lower panel of figure 4 shows absorptance for n_e = 1 × 10^{21} cm^{-3} and layer thicknesses in the $1 \le d \le 100$ µm range and demonstrates that high absorptance extends over a large part of the NIR for the largest values of d while the visible absorptance is still low. An electrochromic device of this type would then switch from NIR-transparent state to a NIR absorbing one as the applied potential is varied.

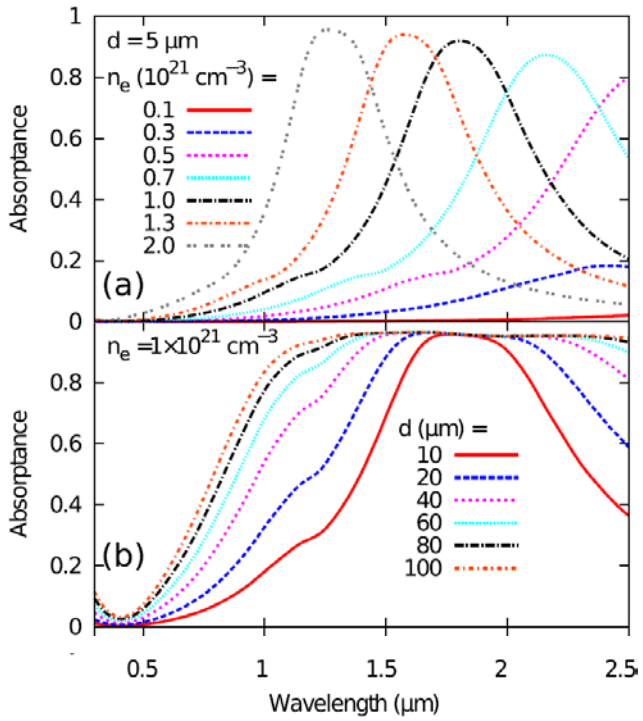

Figure 4. Spectral absorptance for a 5-μm-thick layer with electron densities of 0.1 x $10^{21} \le n_e \le 2 \times 10^{21}$ cm^{-3} (a) as well as for layers with thicknesses of $10 \le d \le 100$ μm and n_e = 1 × 10^{21} cm^{-3} (b). The layer contains 1 vol.% of dispersed spherical ITO nanocrystals. From [37].

Quantitative model calculations using a large number of values of d and n_e were carried out and the resulting data are shown as $T_{lum}(d,n_e)$ *vs.* $T_{sol}(d,n_e)$ in figure 5. It is observed that for each T_{lum} there is a well-defined minimum solar transmittance, denoted $T_{sol,min}$. This can be fitted to a purely empirical expression [37], given by the curve in figure 4, by

$$T_{sol,\min} \approx \alpha + \beta T_{lum} + \gamma T_{lum}^2 + \delta T_{lum}^3 \,, \qquad (10)$$

where α = –1.03, β = 5.94, γ = –9.26 and δ = 5.27. This relation gives an approximate performance limit for a smart window embodying plasmonic NIR electrochromism, based on transparent conducting nanocrystals. It should be noted that eq. (10) represents the optimum solar transmittance in the colored state of an electrochromic device switching from a high T_{sol} to the value in figure 5. The

equation also represents data pertaining to varying electron densities; for example T_{lum} being 0.6, 0.7 and 0.8 corresponds to n_es of 1.52, 1.28 and 0.98 × 10^{21} cm^{-3}, respectively, in the case d = 100 μm. The performance limits are quite impressive; for example a luminous transmittance of 0.6 and 0.8 can be combined with a solar transmittance of 0.35 and 0.5, respectively.

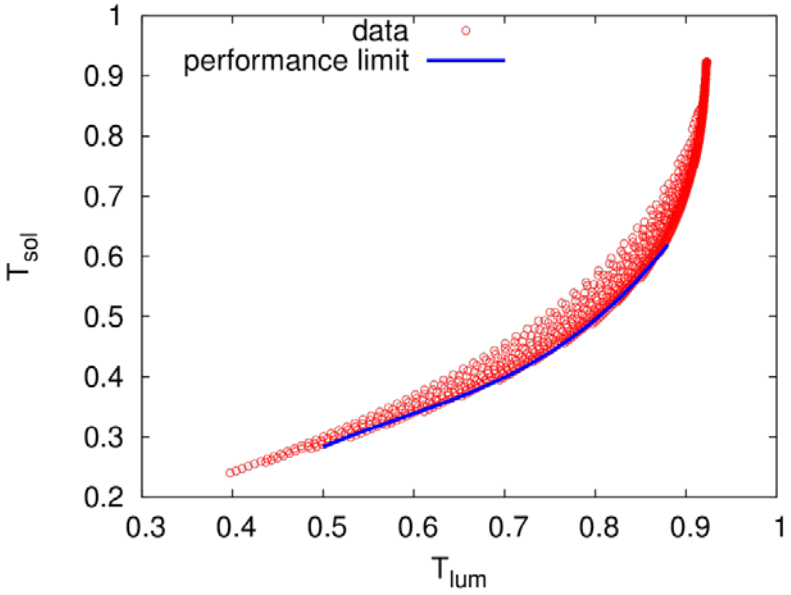

Figure 5. Luminous and solar transmittance (T_{lum} and T_{sol}, respectively) as obtained from model calculations of ITO nanocrystals in a matrix. The curve indicates an approximate performance limit for plasmonic electrochromism. From [35].

5. Thermochromic nanoparticles

Thermochromic (TC) coatings for smart windows as well as the use of TC VO_2 nanoparticles to significantly improve luminous and solar performance of TC films was reviewed in considerable detail by us at the previous INERA Conference in 2014 [38], and this material will not be repeated here. Instead we will describe the basis for, and illustrate the importance of, plasmonic effects for the optical properties of VO_2 nanoparticles. The TC switching in VO_2 occurs between a low temperature phase with semiconducting properties and a high-temperature metallic phase. In the metallic phase, the partly filled conduction band has *d*-character and a description of the dielectric function in terms of the Drude theory (eq. (1)) or extensions thereof appears not to be possible. Nevertheless the dielectric function of VO_2 is sufficiently metallic-like so that a well-defined localized plasma absorption peak appears in the NIR for nanoparticles and nanoparticle composites. Figure 5 shows model calculations [39] of transmittance in the semiconducting and metallic phases for randomly distributed spheroidal VO_2 nanoparticles with various aspect ratios, *m*. The experimental dielectric function of VO_2 in the low and high temperature phases [40,41] was used as input data. The volume fraction of particles was taken to be 1% and the thickness was put to 5 μm. The localized plasma resonance is clearly seen as a dip in the transmittance in figure 5b at a wavelength of about 1200 nm for spherical particles, which shifts to longer wavelengths for oblate spheroids. In comparison, no such transmittance dip is seen for the semiconducting low temperature phase in figure 5a. This contrast leads to a large temperature-dependent modulation of NIR transmittance and a significant TC modulation of solar transmittance [39,41]. For example, large values of T_{lum}, between 0.6 and 0.8, can be combined with a significant thermochromic modulation of T_{sol}, up to 0.25 [41].

(a) (b)

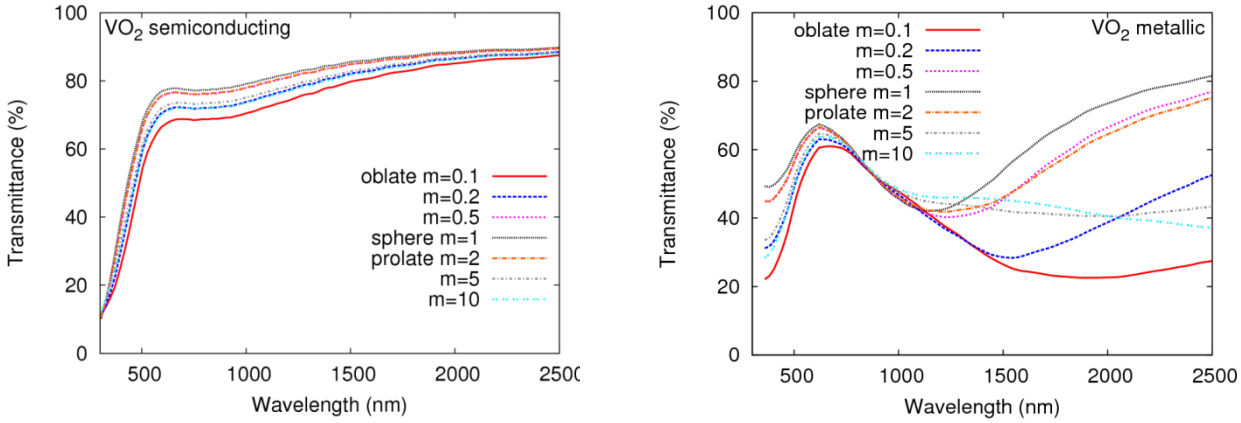

Figure 6. Spectral transmittance for spheroidal VO_2 particles, with the shown aspect ratios *m*, thickness 5 μm and a volume fraction of 0.01, dispersed in a dielectric medium. The spheroids are randomly oriented. Parts (a) and (b) refer to VO_2 in semiconducting and metallic states, respectively. From [39].

6. Conclusion

In this paper we have showed that plasmonic effects are important in a number of applications related to coatings for energy-efficient windows. An elementary treatment of the localized plasma resonance was given and it was shown that nanoparticles of a Drude metal exhibit a Lorentzian absorption peak centered at the resonance frequency. This basic concept was applied to three examples of energy-efficient window coatings. First we showed that very thin gold films with a network structure exhibit a higher solar transmittance than continuous films. When sandwiched between doped oxide layers, thin Au films can be used as transparent contacts for electrochromic devices. Secondly, the field of plasmonic electrochromism takes advantage of the NIR absorption in highly doped conducting oxide nanoparticles. The electron density in the particles comprising a particulate film can be modulated by an external applied potential thereby shifting the localized plasma absorption and giving a pronounced NIR electrochromic effect. By model computations we derived the performance limits of this concept. Thirdly, we showed that VO_2 nanoparticles in the high-temperature metallic phase exhibit a pronounced localized plasma absorption and that this effect leads to nanocomposite thermochromic coatings exhibiting an improved performance.

Acknowledgments

This work was financially supported by the Swedish Research Council for Environment, Agricultural Sciences and Spatial Planning (Formas) and by the European Research Council under the European Community's Seventh Framework Program (FP7/2007–2013)/ERC Grant Agreement No. 267234 ("GRINDOOR"). We are very grateful to Iryna Valyukh and Hans Arwin for ellipsometric measurements and to Enis Tuncer for computing the spectral density function.

This paper was presented at the INERA Conference "Light in Nanoscience and Nanotechnology", Oct. 19-22, 2015, Hissar, Bulgaria. The conference is part of the program INERA REPGOT project of the Institute of Solid State Physics, Bulgarian Academy of Sciences.

References

[1] Stewart M E, Anderton C R, Thompson L B, Maria J, Gray S K, Rogers J A and Nuzzo R G 2008 *Chem. Rev.* **108** 494-521
[2] Anker J N, Hall W P, Lyandres O, Shah N C, Zhao J and van Duyne R P 2008 *Nat. Mater.* **7** 442-53
[3] Antosiewicz T J and Apell S P 2015 *RSC Adv.* **5** 6378-84

[4] Wang P, Huang B, Dai Y and Whangbo M-H 2012 *Phys. Chem. Chem. Phys.* **14** 9813-25
[5] Zhang X, Chen Y L, Liu R-S and Tsai D P 2013 *Rep. Prog. Phys.* **76** 046401
[6] Pillai S, Catchpole K R, Trupke T and Green M A 2007 *J. Appl. Phys.* **101** 093105
[7] Catchpole K R and Polman A 2008 *Opt. Expr.* **16** 21793-800
[8] Winans J D, Hungerford C, Shome K, Rothberg L J and Fauchet P M 2015 *Opt. Expr.* **23** A92-A105
[9] Hägglund C, Zeltzer G, Ruiz R, Thomann I, Lee H-B-R, Brongersma M L and Bent S F 2013 *Nano Lett.* **13** 2252-7
[10] Maxwell Garnett J C 1904 *Phil. Trans Roy. Soc. London* A **203** 385-420
Maxwell Garnett J C 1906 *Phil. Trans Roy. Soc. London* A **205** 237-88
[11] Mie G 1908 *Ann. Phys. (Leipzig)* **330** 377-445
[12] Noguez C 2007 *J. Phys. Chem.* C **111** 3806-19
[13] Roman-Velazquez C E, Noguez, C and Barrera R G 2000 *Phys. Rev. B* **61** 10427-36
[14] Apell S P, Giraldo J and Lundqvist S 1990 *Phase Transitions* **24-26** 577-604
[15] Naik G V, Schroeder J L, Ni X, Kildishev A V, Sands T D and Boltasseva A 2012 *Opt. Mater. Expr.* **2** 478-89
[16] Naik G V, Kim J and Boltasseva A 2011 *Opt. Mater. Expr.***1** 1090-9
[17] Blaber M G, Arnold M D and Ford M J 2010 *J. Phys: Condens. Matter* **22** 143201
[18] Wooten F 1972 *Optical Properties of Solids* (New York: Academic)
[19] Gerlach E and Grosse P 1977 *Festkörperprobleme* **17** 157-93
[20] Lindhard J 1954 *Kgl. Danske Videnskab. Selskab. Mat.-Fys. Medd.* **28** 8
[21] Hamberg I and Granqvist C G 1986 *J. Appl. Phys.* **60** R123-59
[22] Azzam R M and Bashara N M 1977 *Ellipsometry and Polarized Light* (Amsterdam: North-Holland)
[23] Genzel L and Martin T P 1973 *Surf. Sci.* **34** 33-49
[24] Granqvist C G and Hunderi O 1978 *Phys. Rev. B* **18** 2897-906
[25] Bergman D J 1978 *Phys. Rep.* **43** 377-407
[26] Tuncer E 2010 *Materials* **3** 585-613
[27] Tuncer E 2005 *Phys. Rev. B* **71** 012101
[28] Tuncer E and Niklasson G A 2008 *Opt. Commun.* **281** 4374-9
[29] Granqvist C G 2007 *Sol. Energy Mater Sol. Cells* **91** 1529-98
[30] Lansåker P C, Backholm J, Niklasson G A and Granqvist C G 2009 *Thin Solid Films* **518** 1225-9
[31] Lansåker P C, Tuncer E, Valyukh I, Arwin H, Granqvist C G and Niklasson G A 2013 *Progr. Electromagn. Res. Symp. Proc.*, (Stockholm, Sweden, Aug 12–15, 2013) 443-7
[32] Garcia G, Buonsanti R, Runnerstrom E L, Mendelsberg R J, Llordes A, Andres A, Richardson T J and Milliron D J 2011 *Nano Lett.* **11** 4415-20
[33] Berggren L and Niklasson G A 2001 *J. Appl. Phys.* **90** 1860-3
[34] Triana C A, Granqvist C G and Niklasson G A 2015 *J. Appl. Phys.* **118** 024901
[35] Llordes A, Garcia G, Gazquez J and Milliron D J 2013 *Nature* **500** 323-6
[36] Ginley D S, Hosono H and Paine D C (ed.) 2010 *Handbook of Transparent Conductors*, (New York: Springer Science+Business).
[37] Li S-Y, Niklasson G A and Granqvist C G 2012 *Appl. Phys. Lett.* **101** 071903
[38] Niklasson G A, Li S-Y and Granqvist C G 2014 *J. Phys.: Conf. Ser.* **559** 012001
[39] Li S-Y, Niklasson G A and Granqvist C G 2010 *J. Appl. Phys.* **108** 063525
[40] Mlyuka N R, Niklasson G A and Granqvist C G *Phys. Stat. Sol.* A **206** 2155-60
[41] Li S-Y, Niklasson G A and Granqvist C G 2014 *J. Appl. Phys.* **115** 053513